geoconvention
Calgary • Canada • May 15-19 2017

Conformal mapping for RTM from topography

Fernanda Carozzi, Amsalu Y. Anagaw and Mauricio D. Sacchi

Signal Analysis and Imaging Group (SAIG) and Department of Physics, University of Alberta

Summary

Seismic migration from topographic surfaces using finite difference approximation suffers from numerous drawbacks. The main one is adjusting the stencils to an irregular computational grid. To overcome this problem, static-corrections are frequently applied but can result in degraded images for areas with complex topography. In this paper, we consider a coordinate transformation to tackle the problem of migration from topography. The transformation is designed to map a stretched coordinate system conformal to the undulated surface into a Cartesian one. Through the transformation both forward modelling and imaging (RTM) algorithms can be properly applied. We present a numerical example to highlight the advantages of this method for land seismic data.

Introduction

Conventional migration of land seismic data from an irregular surface requires pre-processing due to the presence of distorted wavefields. On one hand, conventional time shift for static corrections are insufficient in the presence of steep elevations and complex near surface velocity structures. On the other hand, Reverse Time Migration (RTM) based on finite difference approximation schemes results in degraded images bearing severe numerical artifacts.

In our work, we introduce a finite-difference (FD) discretization scheme that solves the wave equation without the needs of additional statics correction. We implement a mapping from a stretched curvilinear grid conformal to the free surface to a Cartesian grid (Fornberg, 1988; Tessmer et al., 1992; Hestholm and Ruud, 1994; Shragge, 2016). Discretization is accomplished through FD stencils using velocity-stress formulation on a staggered grid system (Virieux, 1986). Finally, synthetic numerical results for a 2D acoustic model are presented to highlight the advantages of using this method for imaging land seismic data.

Theory

From wave equation propagation theory in 2D acoustic media, a velocity-stress formulation is stated by the following system of first order partial differential equations

$$\rho \frac{\partial v_x}{\partial t} = \frac{\partial p}{\partial x} \tag{1}$$

$$\rho \frac{\partial v_z}{\partial t} = \frac{\partial p}{\partial z} \tag{2}$$

$$\frac{\partial p}{\partial t} = \lambda \left(\frac{\partial v_x}{\partial x} + \frac{\partial v_z}{\partial z} \right), \tag{3}$$

where ρ is the medium density, v_i are the components of the velocity, λ is a Lamé parameter and p is the pressure.

In order to handle irregular surfaces, we adopt a non-Cartesian generalized curvilinear system. The coordinate system is bounded in the vertical direction by the topography. Below the topographic surface, the undulations of the x_1-axis decrease linearly with depth, becoming flat at the bottom of the system. Horizontally, the system is bounded by $x_1 = 0$ and $x_1 = x_{max}$.

To discretize the first-order partial differential equations 1 to 3 in a staggered FD scheme, a rectilinear grid is needed. For the topographic surface scenario, and following Hestholm and Ruud (1994), we use a linear mapping from a rectangular coordinate system (ε, η) to the curved or stretched coordinate system (x, z) conformal to the rugged surface

$$\begin{aligned} x(\varepsilon,\eta) &= \varepsilon \\ z(\varepsilon,\eta) &= \frac{\eta}{\eta_{max}} z_0(\varepsilon)\,, \end{aligned} \tag{4}$$

where $z_0(\varepsilon)$ is the topographic function. The rectangular grid is bounded horizontally by $\varepsilon = 0$ and $\varepsilon = \varepsilon_{max}$, and vertically by $\eta = 0$ and $\eta = \eta_{max}$.

Next, we assume that the curved grid previously defined is embedded on a Cartesian coordinate system where the velocity-stress formulation (equations 1 to 3) is valid. Thus, using chain rule, we obtain the following first-order partial differential equations in the numerical grid

$$\rho \frac{\partial v_x}{\partial t} = \frac{\partial p}{\partial \varepsilon}\frac{\partial \varepsilon}{\partial x} + \frac{\partial p}{\partial \eta}\frac{\partial \eta}{\partial x} \tag{5}$$

$$\rho \frac{\partial v_z}{\partial t} = \frac{\partial p}{\partial \varepsilon}\frac{\partial \varepsilon}{\partial z} + \frac{\partial p}{\partial \eta}\frac{\partial \eta}{\partial z} \tag{6}$$

$$\frac{\partial p}{\partial t} = \lambda \left(\frac{\partial v_x}{\partial \varepsilon}\frac{\partial \varepsilon}{\partial x} + \frac{\partial v_x}{\partial \eta}\frac{\partial \eta}{\partial x} + \frac{\partial v_z}{\partial \varepsilon}\frac{\partial \varepsilon}{\partial z} + \frac{\partial v_z}{\partial \eta}\frac{\partial \eta}{\partial z} \right)\,, \tag{7}$$

where

$$\begin{aligned} \frac{\partial \varepsilon}{\partial x} &= 1 \\ \frac{\partial \varepsilon}{\partial z} &= 0 \\ \frac{\partial \eta}{\partial x} &= -\frac{\eta}{z_0(\varepsilon)}\frac{\partial z_0(\varepsilon)}{\partial \varepsilon} \\ \frac{\partial \eta}{\partial z} &= \frac{\eta_{max}}{z_0(\varepsilon)}\,. \end{aligned} \tag{8}$$

The previous set of equations can be solved using forth order in space and second order in time staggered FD stencils.

Finally, RTM is implemented in the same rectangular coordinate system using the velocity-stress formulation. We adopt the source normalized imaging condition Claerbout (1971)

$$I(x,z) = \sum_s \frac{\sum_t S(x,z,t)R(x,z,t)}{\sum_t S(x,z,t)S(x,z,t) + \nu}\,, \tag{9}$$

where s denotes the number of sources, and ν is a stabilizing parameter that prevents dividing by zero. The fields $S(x,z,t)$ and $R(x,z,t)$ are the source wavefield computed by forward modeling and the receiver wavefield computed by reverse-time extrapolation, respectively.

Examples

In order to asses the performance of the proposed method, we present a numerical experiment where we adopt the Marmousi velocity model. The model is discretized on a $2301\ x\ 751$ grid with a uniform spacing of 4 m in vertical and horizontal directions (Figure 1). Time stepping is 0.0002 s. A total of 12 sources and 2400 receivers are considered in our example. Sources are placed one grid block below the free surface. In addition, we apply Perfectly Matching Layers (PML) boundary conditions

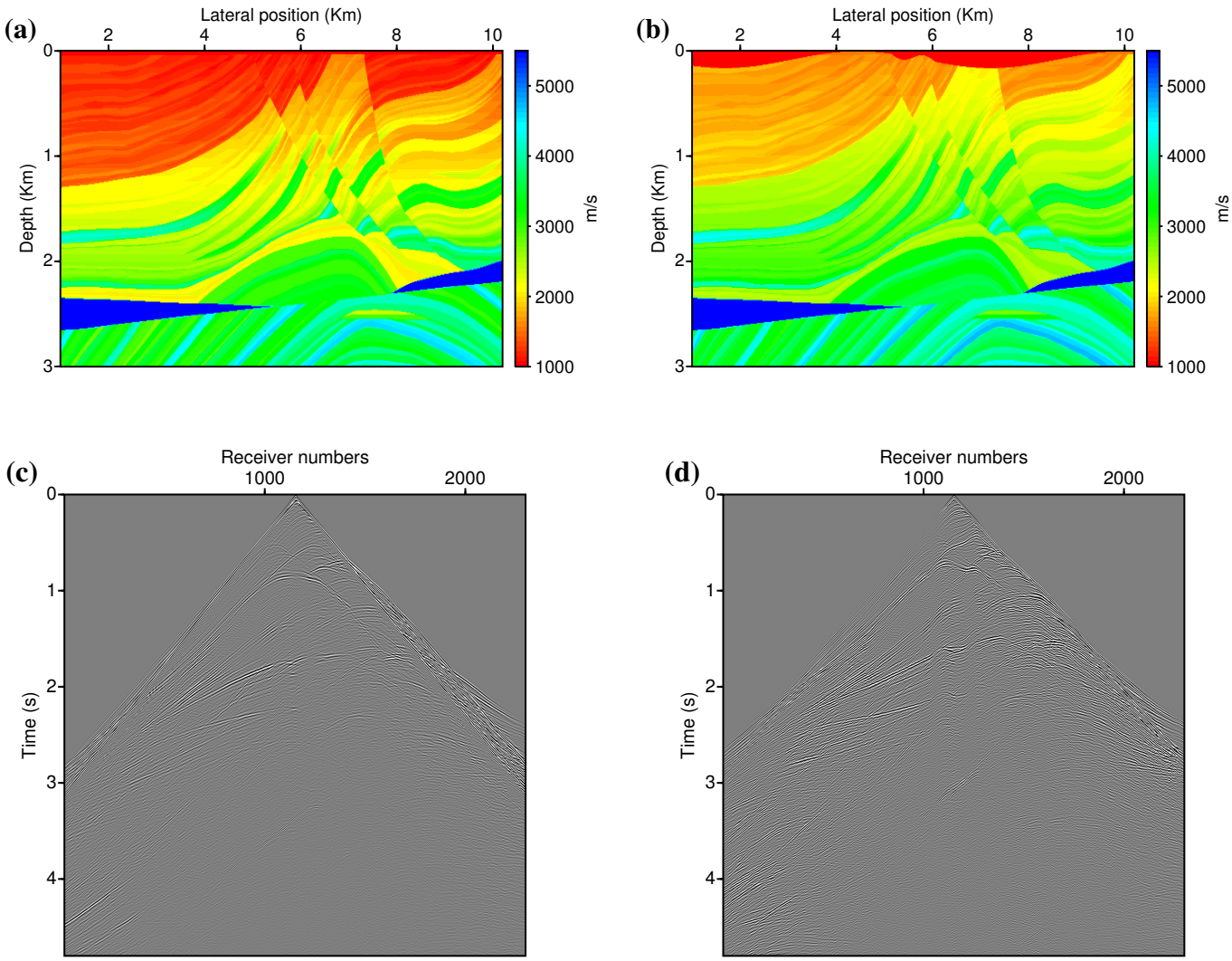

Figure 1: Marmousi velocity model without topography (a) and with topography (b). (c) and (d) Shot gather from models (a) and (b), respectively.

(Berenger, 1994) to absorb undesired reflections from boundaries. Using such conditions we mimic absorbing outgoing waves at the numerical border of the modelled volume. In contrast, for the upper surface we apply a free surface boundary condition to mimic land acquisition conditions.

In Figure 1(a), a flat free surface is considered, while in Figure 1(b) the free surface corresponds to a rugged topography. Figures 1(c) and (d) present the corresponding shot gathers for a source placed in the center of the acquisition surface.

Figures 2 (a) and (b) display the corresponding RTM images. These figures demonstrate that our scheme is properly handling not only the presence of complex structures, but also the presence of topography avoiding the propagation of numerical artifacts.

Conclusion

We presented a 2D acoustic imaging subsurface method that handles rugged topographic surfaces. The proposed technique performs a coordinate transformation from a curved system conformal to a

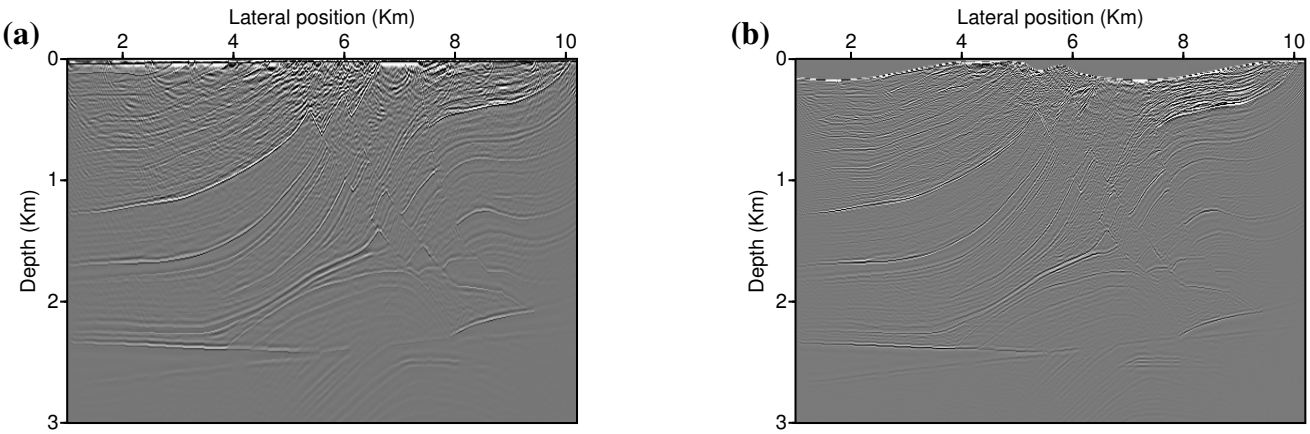

Figure 2: (a) RTM image obtained for the Marmousi velocity model adopting a flat surface (b) RTM image obtained from topography with the proposed method.

rugged surface into a Cartesian one. In this new mesh we solved the first order velocity-stress wave propagation problem. We successfully imaged a complex structure via RTM. The FD technique uses 4th order in space and 2nd order in time staggered stencils. The presented numerical examples highlight the successful application of RTM to data with rugged topographic surface and complex subsurface geology.

Acknowledgements

The authors are grateful to the sponsors of Signal Analysis and Imaging Group (SAIG) at the University of Alberta for their continued support.

References

Berenger, J. P., 1994, A perfectly matched layer for the absorption of electromagnetic waves: Journal of computational physics, **114**, 185–200.
Claerbout, J. F., 1971, Toward a unified theory of reflector mapping: Geophysics, **36**, 467–481.
Fornberg, B., 1988, Generation of finite difference formulas on arbitrarily spaced grids: Mathematics of computation, **51**, 699–706.
Hestholm, S., and B. Ruud, 1994, 2D finite-difference elastic wave modelling including surface topography: Geophysical Prospecting, **42**, 371–390.
Shragge, J., 2016, Acoustic wave propagation in tilted transversely isotropic media: Incorporating topography: Geophysics, **81**, C265–C278.
Tessmer, E., D. Kosloff, and A. Behle, 1992, Elastic wave propagation simulation in the presence of surface topography: Geophysical Journal International, **108**, 621–632.
Virieux, J., 1986, P-SV wave propagation in heterogeneous media: Velocity-stress finite-difference method: Geophysics, **51**, 889–901.